



DESIGN AND OPTIMIZATION OF PMSM BY USING THE THERMAL BEHAVIOUR OF FLUID DYNAMICS

S. Radhika*, Dr. M. Marsalin Beno & Dr. R. A. Jaikumar*****

* Research Scholar, St. Peter's University, Avadi, Chennai, Tamilnadu

** Professor & Head, Department of Electrical & Electronics Engineering,
St. Xavier's Catholic College of Engineering, Kanyakumari, Tamilnadu
Formerly Principal, Athwaitha Mission Engineering College, Bihar

Abstract:

One of the efficient gadgets possessing magnificent scope for the enhancement of energy efficiency is the electrical motor. Amid, several kinds of electrical motors, Permanent magnet synchronous motors are widely employed in countless sophisticated applications. This phenomenon has enabled it to be shortlisted for our investigation, which predominantly centres on the thermal character of the Permanent Magnet Synchronous Motor (PMSM), which is designed and replicated in a Computational Fluid Dynamics Software ANSYS FLUENT-13. The heat transfer inside the motor is assessed for diverse functional constraints like inlet velocity, ambient temperature, air gap thickness, heat flux, and convective heat transfer coefficient. The optimum conditions to be preserved to perk up the heat dissipation pace and to dwindle down the highest temperature are forecast. It is pertinent to note that the forecasts from the analyses closely resemble those gathered from literary community, thereby authenticating the aptness of the assessment.

Keywords: Permanent Magnet Synchronous Motor, Convective Heat Transfer Coefficient, Computational Fluid Dynamics, Air Gap Thickness & Heat Flux.

1. Introduction:

The yester years have watched with gazing eye the amazing phenomenon of electrical power generation from renewable energy sources, like wind in view of the eco-issues and dearth of time-honoured energy source in the days to dawn. Of recent attraction is the rise of permanent magnet synchronous generator (PMSG) as the effective tool for wind power generating system. [1] They are gaining zooming significance for special drive applications. From times immemorial, they are mainly used for small drives such as servo applications. But the advent of recent era has witnessed PMSM expanding its zooming relevance in diverse domains like traction, automobiles, and so on. One of the effective means of managing AC motors for inconsistent speed applications is the open loop scalar control, which characterizes the most well-known control strategy of squirrel cage AC motors.[2] Utilization of PMSMs as traction motors is widely prevalent in electric or hybrid road vehicles, except in the case of rail vehicles. [3]

Since the inception of electric motors and resultant urge to step up their efficiencies, many hassles have erected roadblocks in the pathway of machines in the form of heating menaces. Certain segments the machines are capable of attaining the noteworthy and barred temperatures leading their corrosion. The major segments in this regard comprise the winding insulators, the bearings or the magnets. These latter are especially sensitive to lofty temperatures as they lose a significant part of their magnetization when exposed to exceedingly elevated temperature. With an eye on maintaining the optimal stipulations guaranteeing the superb functioning of the motor, it is essential to effectively comprehend and thereby manage the thermal character of these motors. This ultimately results in the indispensable necessity for the superlative

design of coolers to guarantee that the operating temperatures are within the desirable restrictions of used materials. [4]

The design of highly efficient electrical machines is an aggressive and multi inhibited assignment which has to precisely evaluate the electrical, magnetic, and thermal loads to yield utmost material utilization. In this backdrop, optimal design has obviously emerged as an effective method integrating electrical and mechanical talents together with thermal and fluid dynamic skills. In addition, in the case of modern machine layouts, typical evaluation techniques have lost all relevance [5]. An effective approach of analyzing the thermal character of electric machines is mainly dependent on thermal equivalent circuit networks envisaging a 1-D or 2-D heat flow in the electric machine. [6] For the evaluation of a thermal equivalent circuit, the utmost taxing task is the parameterization of the heat transfer coefficients of the convective models. [7] For permanent magnet synchronous machines, the situation is completely different. As the rotor is not equipped with any sort of cooling blades, the internal air stream is rather marginally developed vis-a-vis the induction machines [8]. The underlying intention behind this document is to make an effective evaluation of the heat production and transfer inside the motor and the renovation of the design to step up the heat dissipation tempo together with shrinking the utmost temperature by means of investigation employing CFD.

2. Related Works:

Yulia Alexandrova *et al.*[9] have amazingly offered a account on the expansion of a novel type of generator for wind energy, which is a compact, high-power, direct-drive permanent magnet synchronous generator (DD-PMSG) employing direct liquid cooling (LC) of the stator windings to cut down the Joule heating damages. The cooling feat of the liquid cooled tooth-coil model is envisaged by means of finite element evaluation. An instrumented cooling loop highlighting a pair of LC tooth-coils entrenched in a lamination stack is made and laboratory investigated to corroborate the analytical model. Forecast and estimated outcomes are found to be in harmony, substantiating the forecast reasonable function of the LC DD-PMSG cooling technology technique altogether.

Li Liu *et al.* [10] have marvellously launched an intelligent model parameter identification technique by means of particle swarm optimization (PSO), and gifted computational approach dependent on stochastic investigation which has proved its mettle as a multitasking and proficient device for the related intricate engineering issue. By deftly blending both replication and investigation, this document delves deep into the efficiency in performance of the projected method in recognition of PMSM model constraints. Specially, stator resistance and load torque disturbance are remarkably recognised in the PMSM application. Even though the PMSM is offered, it is usually relevant to identical categories of electrical motors together with other vibrant systems equipped with nonlinear model structure.

Fabrizio Marignetti *et al* [11] have fabulously formulated a novel thermal evaluation of an axial flux synchronous permanent-magnet machine (AFSPM) with a core of soft magnetic composite (SMC) material. The temperature allocation is effected by means of a coupled thermal and fluid dynamic finite-element method. The evaluation covers two different 2-D techniques and aptly analyzes their outcomes to tentative tests. Takashi Kosaka *et al.*[12] have competently tabled a hybrid excitation motor for a main spindle drive in end- and face-milling tools, which is executed at an elevated speed of 50 000 r/min. The innovative motor is endowed with a permanent magnet along with the

field coil which enables field declining and field-boosting controls by ignoring the permanent magnet demagnetization. Moreover, the total losses of iron and copper of the motor at the end-milling function is considerably cut down by the field-declining control. The 3-D finite-element-method-based design evaluations on the novel motor for the target application are effectively established.

Fabrizio Marignetti *et al.* [13] have fantastically made probes into the thermal character of axial flux synchronous permanent-magnet machines (AFSPMMs) by means of a 3-D thermal-magnetic finite-element analysis (FEA). The author presents a systematic method to magneto thermal FEA. The contemplated axial flux machine is wound on a soft magnetic compound core. The estimation of thermal field is carried out through a coupled thermal and fluid-dynamical model based on FEA, where the thermal sources are gathered from a dc current flow model and a magneto static model. This document effectively endeavours an evaluation on the execution of the finite-element method (FEM) model. Replication results are furnished and, with a view to authenticate the model, the replicated surface temperature increase of the motor parts is assets by test outcomes data.

3. Process Modelling of Permanent Magnet Synchronous Motor:

3.1 Three significant modelling step involve in process modelling are as follows;

- Pre-Processing
- Solver Processing
- Post Processing

3.1.1 The present model assumes that

- i. The working fluid is air and its properties remain constant
- ii. The flow is 3D, steady - state, incompressible, and turbulent.
- iii. The thermal constant resistance is negligible at the solid-solid since the flow is highly turbulent, a renormalized group (RNG) k-ε model was chosen for the flow analysis.

$$\text{Fluid region, Continuity: } \frac{\partial}{\partial x_i} (\rho u_i) = 0 \quad (1)$$

$$\text{Momentum: } \frac{\partial}{\partial x_j} (\rho u_i u_j) = -\frac{\partial p}{\partial x_i} + \frac{\partial}{\partial x_j} \left[(\mu + \mu_t) \frac{\partial u_i}{\partial x_j} \right] \quad (2)$$

Turbulent kinetic energy:

$$\frac{\partial}{\partial x_j} (\rho u_j k) = \frac{\partial}{\partial x_j} \left[\left(\mu + \frac{\mu_t}{\sigma_k} \right) \frac{\partial k}{\partial x_j} \right] + G_k - \rho \epsilon \quad (3)$$

Turbulent kinetic energy dissipation:

$$\frac{\partial}{\partial x_j} (\rho u_j \epsilon) = \frac{\partial}{\partial x_j} \left[\left(\mu + \frac{\mu_t}{\sigma_\epsilon} \right) \frac{\partial \epsilon}{\partial x_j} \right] - C_2 \rho \frac{\epsilon^2}{k + \sqrt{v \epsilon}} \quad (4)$$

$$\text{Energy: } \rho C_p \frac{\partial}{\partial x_j} (u_j T) = k_{eff} \frac{\partial^2 T}{\partial x_j^2} + (\tau_{ij}) \frac{\partial u_i}{\partial x_j} \quad (5)$$

$$\text{Where, } \mu_t = \rho C_\mu \frac{k^2}{\epsilon} \quad (6)$$

$$G_k = 2\mu_t S_{ij} S_{ij} = \mu_t \left(\frac{\partial u_j}{\partial x_i} + \frac{\partial u_i}{\partial x_j} \right) \frac{\partial u_i}{\partial x_j} \quad (7)$$

Solid regions

The following conduction equation was applied to account for the internal heat transfer:

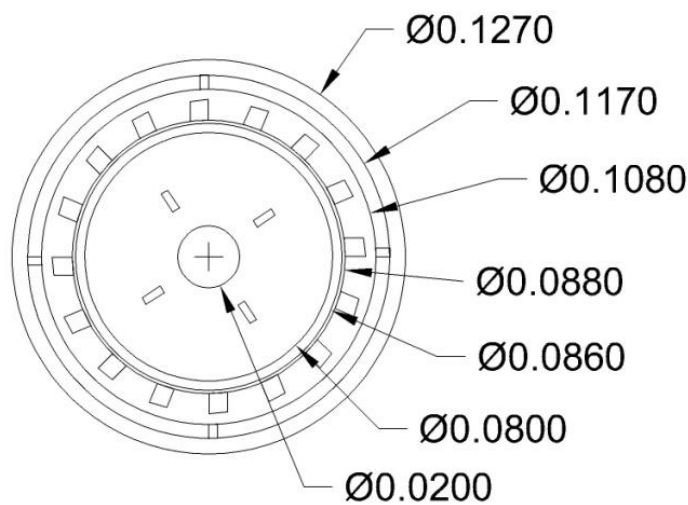
$$k_{sj} \frac{\partial^2 T}{\partial x_j^2} + S_g = 0 \quad (8)$$

Where,

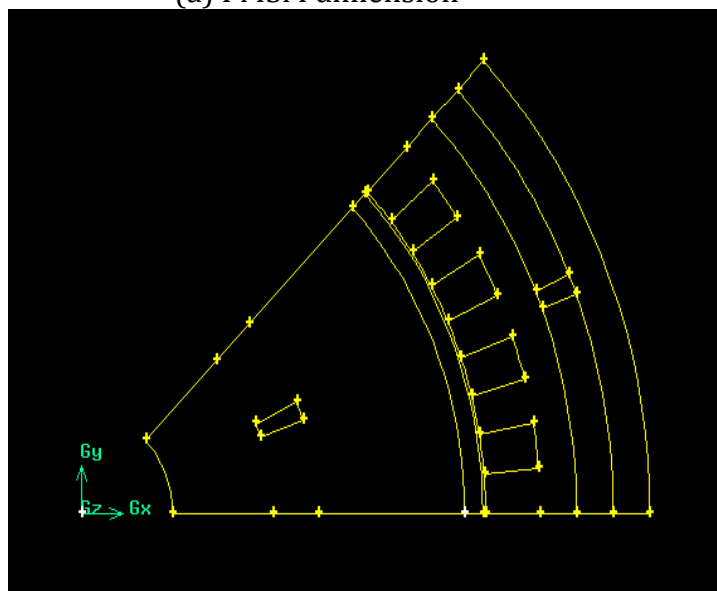
V_w and V_b are volume of winding and bearing, respectively.

3.2 Permanent Magnet Synchronous Motor Modelling:

The 3D model of 1HP Permanent Magnet Synchronous motor is designed by means of the software GAMBIT as illustrated in Figure 1. The dimension of a common Permanent magnet synchronous motor is effectively employed here. It is home to several components like Rotor, Permanent magnet, Air gap, Windings, Magnetic sheet, Air gap to end windings, Frame.



(a) PMSM dimension



(b) GAMBIT

Figure 1: Permanent Magnet Synchronous Motor Modelling

The modules in the interior of the motor are of Standard dimensions. With the objective of scaling down the intricacy of modelling, the 45° cross section of the motor is designed by means of the software GAMBIT as illustrated in Fig.2 and it is evaluated by means of FLUENT.

3.3 Meshing Process:

The Meshing, in essence, represents the procedure of segmenting the overall domain into tiny modules termed as Nodes. The imported model is provided with meshes and limit constraints and, cell zone parameters are formulated. The total number of nodes created amounts to 429748 as depicted in Figure 4.

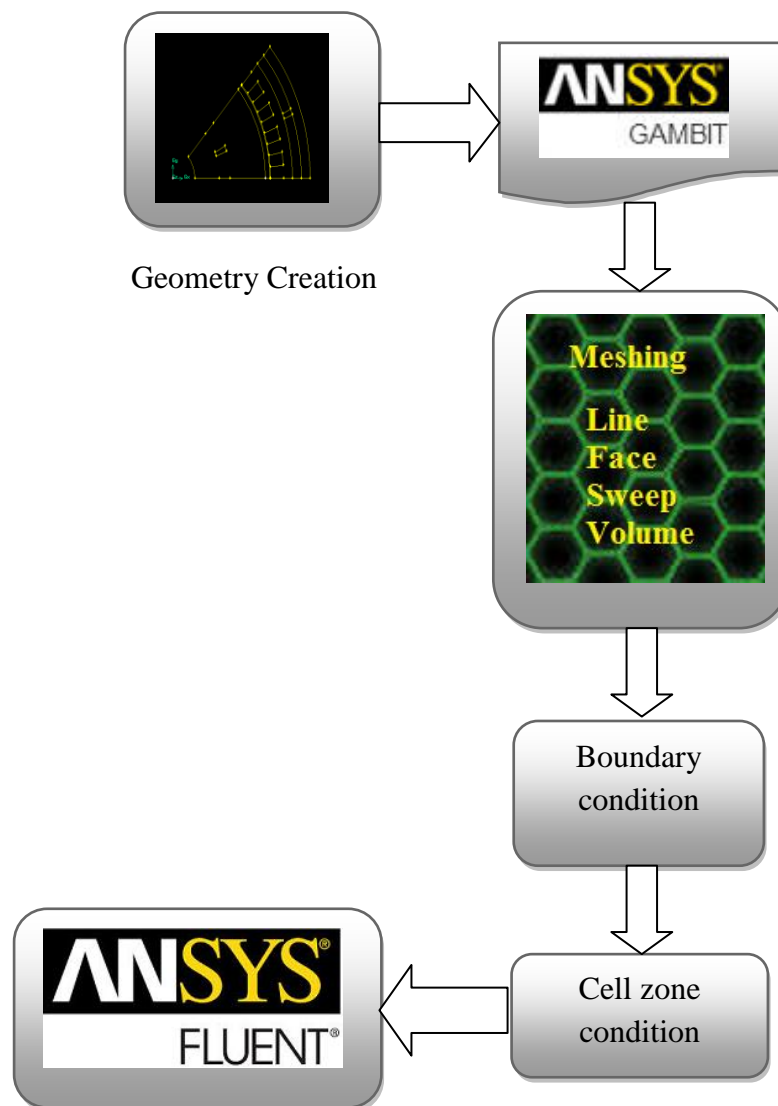


Figure.2 meshing process

3.4 Analysis of PMSM:

The Analysing is done in Ansys Fluent i.e. the solver execution and post processing. The analysing procedure is given in the flowchart which is listed as follows:

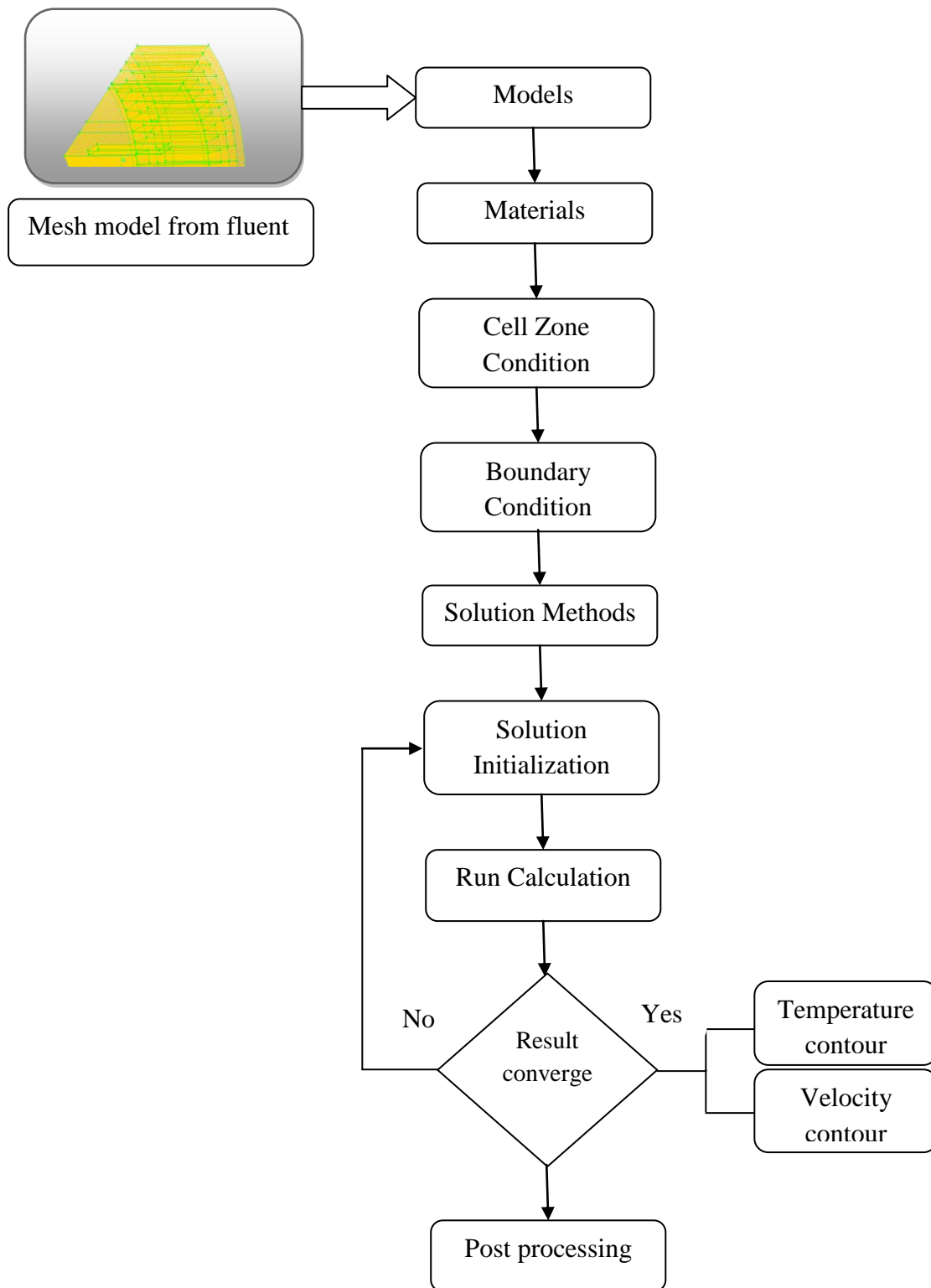


Figure 3: Post processing analysis for PMSM

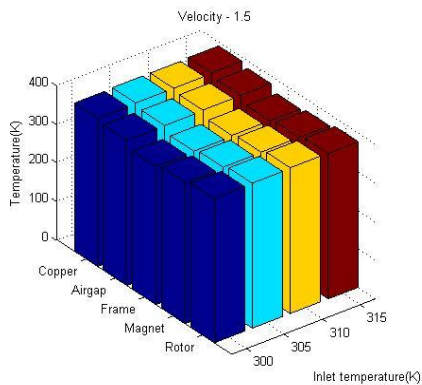
The mesh designed from fluent is adapted and a material configuration is made and executed for cell zone and boundary constraints, thus achieving the solution techniques. These solutions are employed for initialization to work out the procedure. If the achieved outcomes are positive then temperature and velocity contours are

examined. If not, the solution initialization is replicated for attaining positive outcomes after the post processing procedure.

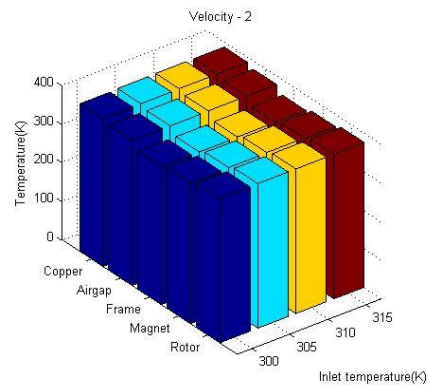
4. Results and Discussion:

Case: 1 (Constant heat flux of copper and magnet ($800\text{w}/\text{m}^2$ and $700\text{w}/\text{m}^2$) having air gap thickness 1.5mm with varying inlet temperature and velocity)

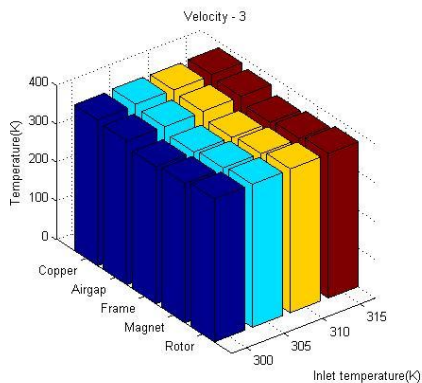
The analysis is done by varying the inlet temperature from 300K to 315K of PMSM at constant heat flux for Copper and Magnet ($800\text{W}/\text{m}^2$ and $700\text{W}/\text{m}^2$ respectively) and constant convective coefficient for Frame ($10\text{W}/\text{m}^2\text{K}$). The thickness of air gap is 1.5mm and the velocity was varied from 1.5m/s to 5m/s.



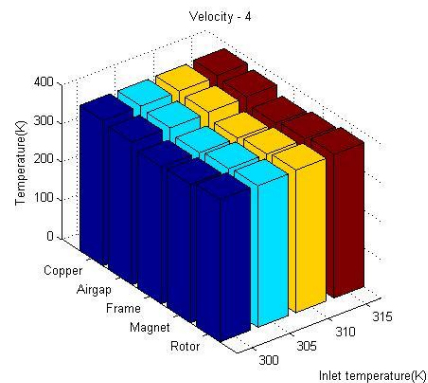
(a) Velocity 1.5



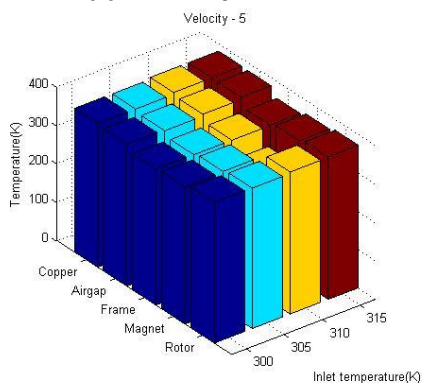
(b) Velocity 2



(c) Velocity 3



(d) Velocity 4



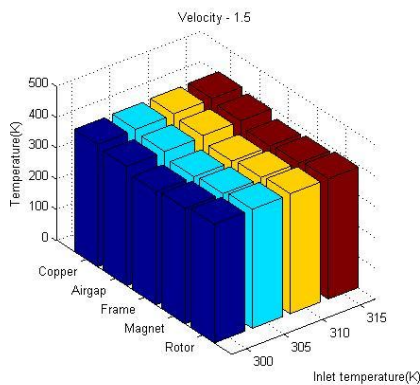
(e) Velocity 5

Figure: 4 Velocity based constant heat flux for Copper and Magnet ($800\text{W}/\text{m}^2$ and $700\text{W}/\text{m}^2$) with air gap thickness 1.5mm

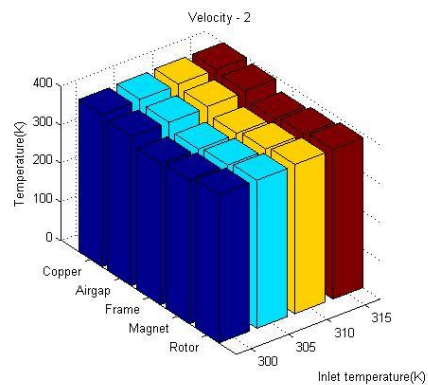
For the ambient temperature of 300K to 315K and for the velocity 1.5 m/s to 5 m/s the sway of component temperature of PMSM at steady heat flux of Copper and Magnet (800W/m² and 700W / m² respectively) is exhibited in Figs. 4 (a), (b), (c), and (d). It is clear from the figure the manner in which the temperature of each component in PMSM changes for several inlet temperature constraints in relation to fluctuating air inlet velocity at steady heat flux. With the enhancement in the inlet temperature, temperature of the component goes up linearly as illustrated in the captioned graphs. It is also seen that copper has an elevated level of temperature of 385K at the velocity 1.5m/s. However, the temperatures of copper and magnet remain within the limit at ambient temperature up to 305K at velocity 2m/s. When there is an enhancement the ambient temperature by 1.63%, the copper temperature is found to fall by 0.527% and magnet temperature by 0.547%. The temperature may be brought down by furnishing superior air velocity, though it entails supplementary energy.

Case: 2 (Constant heat flux of copper and magnet (900w/m² and 800w/ m²) having air gap thickness 1.5mm with varying inlet temperature and velocity)

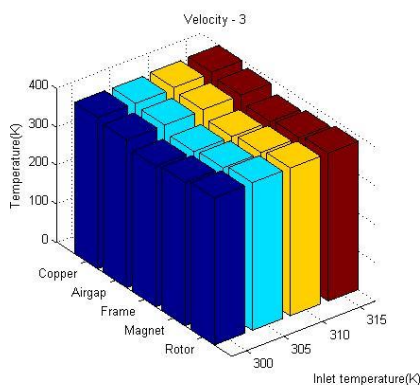
The analysis is done by varying the inlet temperature (300K to 315K) of PMSM at constant heat flux for Copper and Magnet (900W/m² and 800W/m²) and constant convective coefficient for frame (10W/m²K). The thickness of air gap is 1.5mm and the velocity was varied from 1.5m/s to 5m/s.



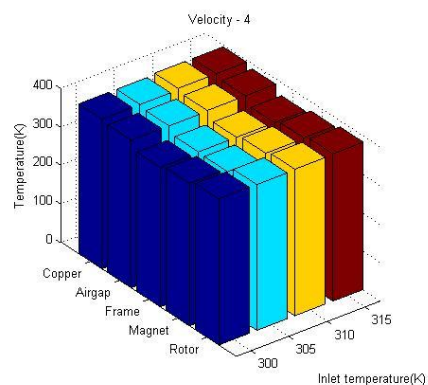
(a) Velocity 1.5



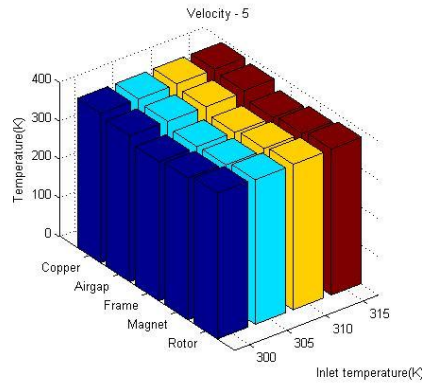
(b) Velocity 2



(c) Velocity 3



(d) Velocity 4



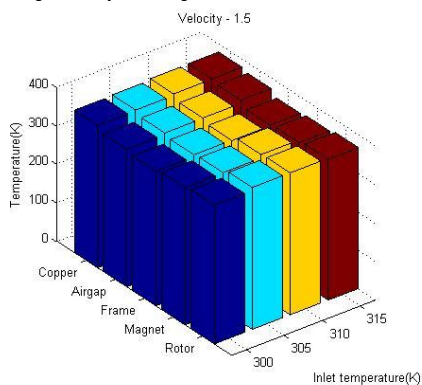
(d) Velocity 5

Figure: 5 Velocity based constant heat flux for Copper and Magnet ($900\text{W}/\text{m}^2$ and $800\text{W}/\text{m}^2$) with air gap thickness 1.5mm

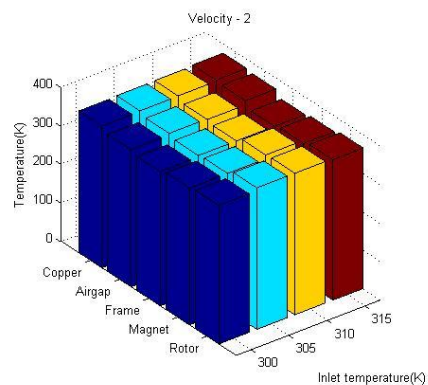
The temperature allocation of several modules of PMSM in respect of fluctuating air velocity and ambient temperature at steady heat flux of Copper ($900\text{W}/\text{m}^2$) and Magnet ($800\text{W}/\text{m}^2$) is beautifully drawn in Figures.5 (a), (b), (c) and (d). It is crystal clear from the figures that the temperature of several modules shrinks considerably when the velocity gets a pick up from 1.5m/s to 3m/s. However the changes are minimal, when the velocity exceeds 3m/s. whereas a step up in the ambient temperature to the tune 1.63% results in the reduction of copper and magnet temperatures by 0.507% and 0.536% respectively. At superior heat flux for copper and magnet, the temperature of modules is well below the limit

Case: 3 (Constant heat flux of copper and magnet ($900\text{w}/\text{m}^2$ and $800\text{w}/\text{m}^2$) having air gap thickness 2mm with varying inlet temperature and velocity)

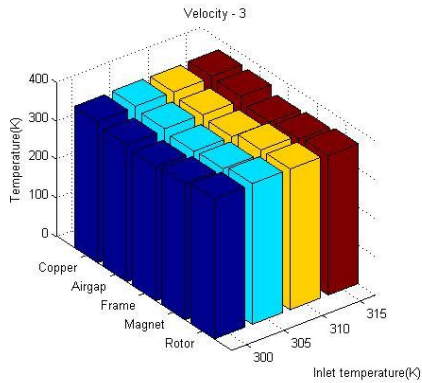
The analysis is done by varying the inlet temperature (300K to 315K) with respect to varying inlet velocity (1.5m/s to 5m/s) of PMSM at constant heat flux for Copper and Magnet ($900\text{W}/\text{m}^2$ and $800\text{W}/\text{m}^2$) at constant convective coefficient for frame ($10\text{W}/\text{m}^2\text{K}$). The thickness of air gap is 2mm.



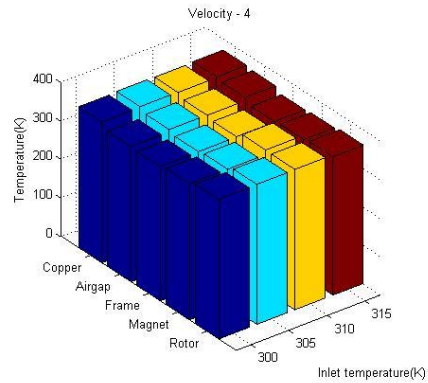
(a) Velocity 1.5



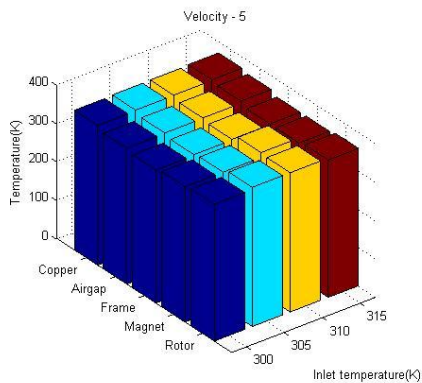
(b) Velocity 2



(c) Velocity 3



(d) Velocity 4



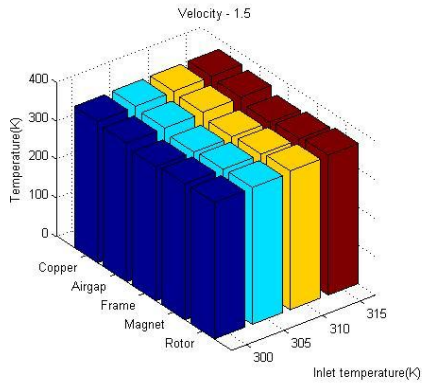
(e) Velocity 5

Figure: 6 Velocity based constant heat flux for Copper and Magnet ($900\text{W}/\text{m}^2$ and $800\text{W}/\text{m}^2$) with air gap thickness 2mm

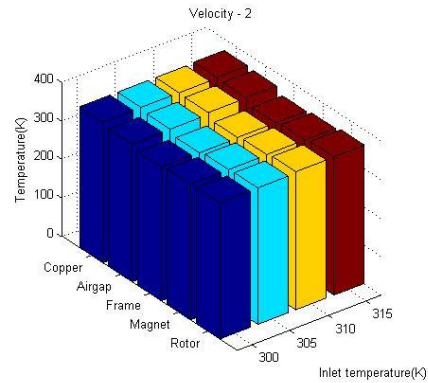
In this investigation the air gap thickness is considerably augmented from 1.5mm to 2 mm and the temperature allocation of several modules of PMSM in respect of fluctuating air velocity and ambient temperature at steady heat flux of Copper ($900\text{W}/\text{m}^2$) and Magnet ($800\text{W}/\text{m}^2$) is well exhibited in Figures 6 (a), (b), (c) and (d). As evident from the graph, at air gap thickness of 2mm, the temperatures of several modules shrink significantly when there is an enhancement in velocity from 1.5m/s to 2m/s. However, the change is negligible for increases in the velocity above 2m/s. At superior heat flux for copper and magnet the temperature of modules are well within the limit at velocity 2m/s and ambient temperature of 300K. When the ambient temperature by 1.63%, the copper temperature decreases by 0.806% and magnet temperature is cut down to the tune of 0.2816%. However, with an enhancement in the air gap thickness the temperature of modules is superior vis-a-vis others.

Case: 4 (Constant heat flux of copper and magnet ($800\text{W}/\text{m}^2$ and $700\text{W}/\text{m}^2$) having air gap thickness 2mm with varying inlet temperature and velocity)

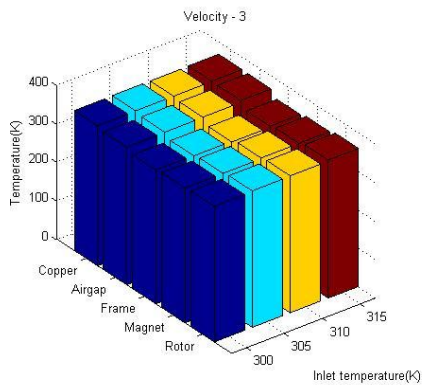
The analysis is done by varying the inlet temperature (300K to 315K) with respect to varying inlet velocity (1.5m/s to 5m/s) of PMSM at constant heat flux for Copper and Magnet ($800\text{W}/\text{m}^2$ and $700\text{W}/\text{m}^2$) at constant convective coefficient for frame ($10\text{W}/\text{m}^2\text{K}$). The thickness of air gap is 2mm.



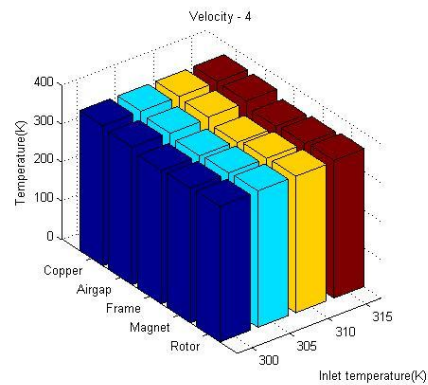
(a) Velocity 1.5



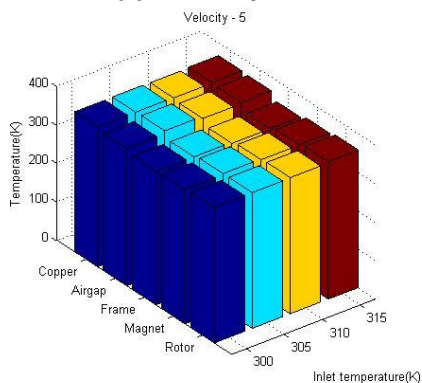
(b) Velocity 2



(c) Velocity 3



(d) Velocity 4



(e) Velocity 5

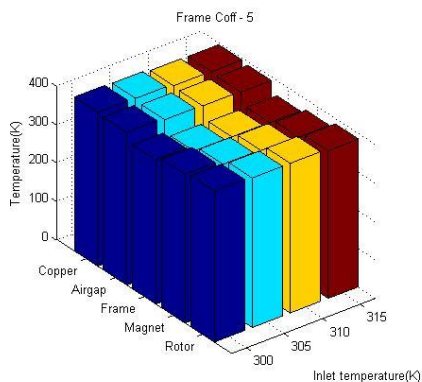
Figure: 7 Velocity based constant heat flux for Copper and Magnet ($800\text{W}/\text{m}^2$ and $700\text{W}/\text{m}^2$) with air gap thickness 2mm

In this evaluation, the air gap thickness is perked up from 1.5mm to 2 mm and the temperature distribution of several segments of PMSM in respect of altering air velocity and ambient temperature at stable heat flux of Copper ($800\text{W}/\text{m}^2$) and Magnet ($700\text{W}/\text{m}^2$) is demonstrated in Figures 7 (a), (b), (c) and (d). It is evident that at air gap thickness of 2mm the temperature of diverse segments shrinks down considerably when the velocity gets enhanced from 1.5m/s to 2m/s though the change is trivial for cases where the velocity exceeds 2m/s. During the course of an enhancement in the ambient temperature around 1.63%, the copper and magnet temperatures dips down by 0.546% and 0.284% respectively. Thus, it is a fact that at a velocity of 2m/s and air

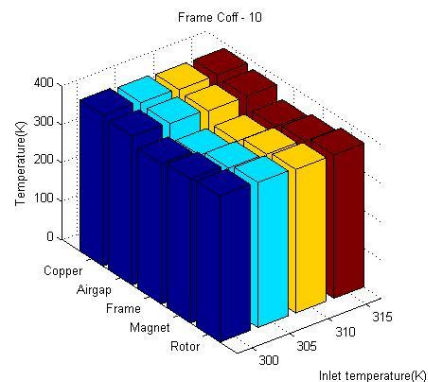
gap thickness of 2mm the temperature of magnet and copper does not go beyond the limit prescribed.

Case: 5 (Convective Coefficient)

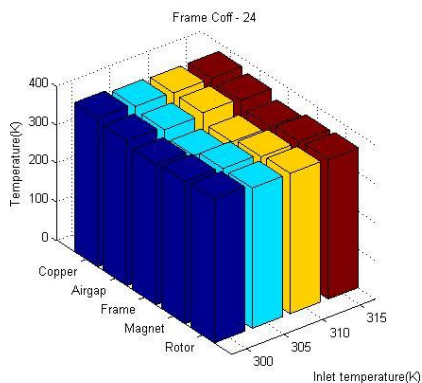
The temperature allocation of several segments of PMSM in terms of unstable Convective Heat transfer Coefficient to the frame is depicted in Figure 8. It is evident from the outcomes that the optimum velocity is 2m/s, air gap thickness 2mm and heat flux for Copper and Magnet (800W/m^2 and 700W/m^2) correspondingly. With these constraints maintaining stability, by duly modifying Convective Coefficient to the Frame, the temperature allocation of diverse segments of PMSM are illustrated in the following Figure 8. The Convective Coefficient values taken into effect are $5\text{W/m}^2\text{K}$, $10\text{W/m}^2\text{K}$, $24\text{W/m}^2\text{K}$ and $32\text{W/m}^2\text{K}$. The heat flux and velocity are preserved at steady values and the ambient temperature gets changed from 300K to 315K.



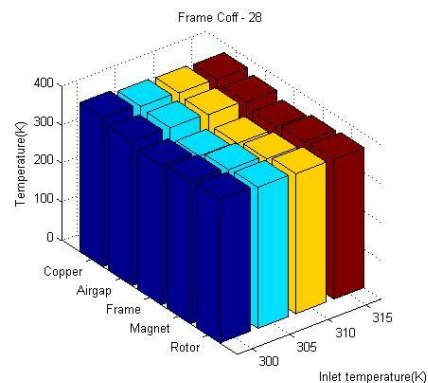
(a) Convective Coefficient 5



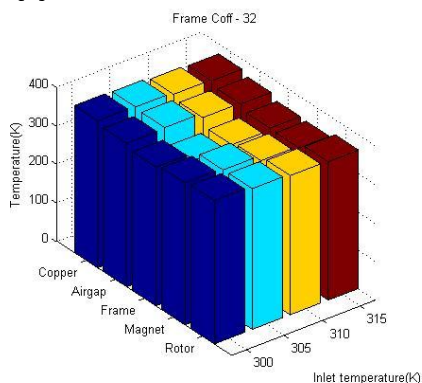
(b) Convective Coefficient 10



(c) Convective Coefficient 24



(d) Convective Coefficient 28



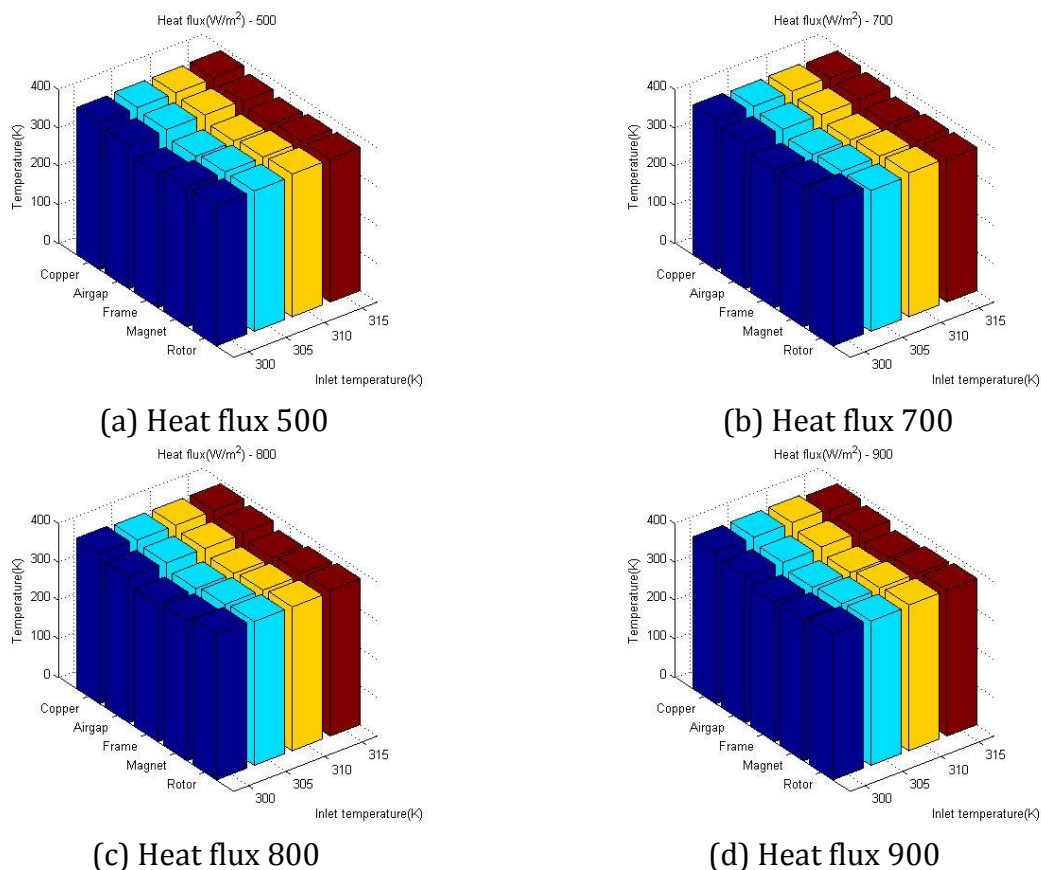
(e) Convective Coefficient 32

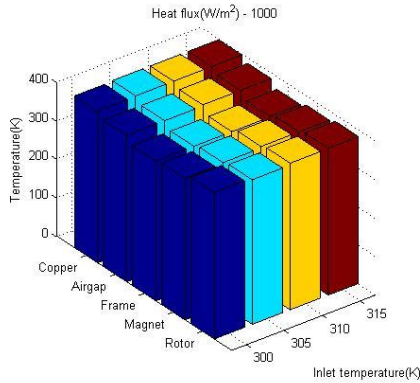
Figure: 8 Velocity based constant heat flux for Copper and Magnet (800W/m^2 and 700W/m^2) with air gap thickness 2mm

Figure 8 explicitly demonstrates the manner in which the temperature of every segment in PMSM alters for several inlet temperature constraints in respect of fluctuating Convective Heat transfer Coefficient for Frame (5 to $32\text{W/m}^2\text{K}$). Figures (a), (b), (c) and (d) make it crystal clear that by enhancing the Convective heat transfer coefficient to the frame for oscillating ambient temperature, the temperature of the segments diminishes linearly, though for effecting higher convective heat transfer coefficient added energy is highly essential. As evident from the figures, the temperature of segments declines sharply up to convective coefficient of $10\text{W/m}^2\text{K}$, and from 10 to $32\text{W/m}^2\text{K}$ their temperature dwindles progressively. And at $h=10\text{W/m}^2\text{K}$ their temperatures does not exceed the limit and thus is the temperature of Copper is 375K and that of Magnet 361K .

Case: 6 (Heat flux)

The temperature distribution of various components of PMSM with respect to varying heat flux to Copper and Magnet (500W/m^2 to 1000W/m^2) is shown in Figure 9. The analyses were carried out at constant velocity of 2m/s , air gap thickness of 2mm and Convective Coefficient of $10\text{W/m}^2\text{K}$.





(e) Heat flux 1000

Figure: 9 Heat flux variation for a constant air gap and different atmospheric temperatures

Figures.9 (a), (b), (c), and (d) evidently characterize how the temperature of each segment of PMSM alters for several inlet temperature situations in respect of fluctuating Heat flux to copper and Magnet (500W/m^2 to 1000W/m^2). And Figure 9 makes it crystal clear that by perking up the Heat flux value to the Copper and Magnet the temperature of the segment can be enhanced. Moreover, for heat flux value of 500 to 800W/m^2 the temperature of segments goes in the northward direction steadily and after 800W/m^2 the segment temperature shoots up swiftly.

4.1 Component's Temperature:

Table 1: Component's Temperature

Components	Lowest Temperature(K)	Highest Temperature(K)	Proposed Temperature(K)
Copper	364	403	403
Magnet	352	380	363
Frame	328	362	330

The Table 1 shows the temperature range of various components of motor such as; these values have been compared with that of the proposed temperature. It is observed that the component temperature lies within the proposed limits.

5. Conclusion:

The evaluation is performed by making due changes in the inlet air velocity from (1.5 - 5) m/s and resultant outcomes demonstrate that at inlet air velocity of 2 m/s the temperature of a variety of modules of PMSM do not exceed the limit. Conversely, at the ambient temperature of 300k the module temperatures park themselves well below projected limits. However, when it is greater than 300K, the module temperatures take a U turn and go beyond the limit. Hence the temperature around the motor has to be maintained below 300K for the superior existence of PMSM. Notwithstanding the saying "higher the air gap, better the cooling", the air gap thickness of 2 mm is deemed to be appropriate. The yielded outcomes underline the fact that elevated heat flux to copper and magnet steps up the module temperature of PMSM. The optimum heat flux for copper and magnet realized from the evaluation are 800W/m^2 and 700W/m^2 correspondingly. By doling out suitable Convective Heat transfer Coefficient to the Frame, module temperature of PMSM can be put under check. As evident from the outcomes, the optimum value of Convective Coefficient yield is $10\text{W/m}^2\text{K}$. Hence appropriate ventilation has to furnish around the motor to restrict the temperature of modules. In view of the constraints in preparing the test system to evaluate the

temperature of several modules of PMSM at various functional situations, just a few constraints are put to examination to authenticate the evaluation. In addition, the inlet and outlet geometry arrangements are adapted to make the model simple for replication. It is highly essential that these parameters are done away with in good time by means of artificial intelligence.

6. References:

1. Yulia Alexandrova, Robert Scott Semken and Juha Pyrhönen, "Permanent magnet synchronous generator design solution for large direct-drive wind turbines: Thermal behavior of the LC DD-PMSG", *Applied Thermal Engineering*, Vol.65, No.2, pp.554-563, 2014
2. Li Liu, Wenxin Liu, David A. Cartes, "Particle swarm optimization-based parameter identification applied to permanent magnet synchronous motors", *Engineering Applications of Artificial Intelligence*, Vol.21, No.7, pp.1092-1100, 2008
3. Fabrizio Marignetti and Vincenzo Delli Colli, "Thermal Analysis of an Axial Flux Permanent-Magnet Synchronous Machine", *IEEE Transactions on Magnetics*, Vol. 45, No. 7, pp.2970-2975, July 2009
4. Takashi Kosaka, Muthubabu Sridharbabu, Masayoshi Yamamoto, and Nobuyuki Matsui, "Design Studies on Hybrid Excitation Motor for Main Spindle Drive in Machine Tools", *IEEE Transactions On Industrial Electronics*, Vol. 57, No.11, pp.3807-3813 November 2010
5. Fabrizio Marignetti, Vincenzo Delli Colli and Yuri Coia, "Design of Axial Flux PM Synchronous Machines Through 3-D Coupled Electromagnetic Thermal and Fluid-Dynamical Finite-Element Analysis", *IEEE Transactions On Industrial Electronics*, Vol. 55, No. 10, pp.3591-3601 October 2008
6. Belakehal Benalla and Bentounsi, "Power maximization control of small wind system using permanent magnet synchronous generator", *Power maximization control of small wind system using permanent magnet synchronous generator*, Vol.12, No.2, pp307-319, 2009
7. Marek Stulrajter, Valeria Hrabovcova and Marek Franko, "Permanent Magnets Synchronous Motor Control Theory", *Journal of Electrical Engineering*, Vol.58, No.2, pp.79-84, 2007
8. Radovan dolecek, jaroslav novak, ondrej cerny, "Traction Permanent Magnet Synchronous Motor Torque Control with Flux Weakening ", *Radio Engineering*, Vol.18, No.4, pp.601-605, 2009
9. Souhil Seghir-Oualil, Souad Harmand and Daniel Laloy, "Study of the thermal behavior of a synchronous motor with permanent magnets ", *International Journal of Engineering (IJE)*, Vol.3, No.3, pp.229-256, 2010
10. Fabrizio Marignetti, Vincenzo Delli Colli and Yuri Coia, "Design of Axial Flux PM Synchronous Machines Through 3-D Coupled Electromagnetic Thermal and Fluid-Dynamical Finite-Element Analysis", *IEEE Transactions On Industrial Electronics*, Vol. 55, No. 10, pp.3591-3601, October 2008
11. Shenkman and Chertkov, "Experimental method for synthesis of generalized thermal circuit of polyphase induction motors," *IEEE Trans. Energy Convers.*, vol. 15, no. 3, pp. 264–268, Sep. 2000.
12. F. Marignetti, Delli Colli, and Coia, "Design of axial flux pm synchronous machine through 3-D coupled electromagnetic thermal and fluid –dynamical finite-element analysis", *IEEE Trans. Ind. Electron.*, vol.55, no.10, pp.3591-3601, oct-2008.

13. Christian Jungreuthmayer, Thomas Bauml, Oliver Winter, Hansjorg Kapeller, Anton Haumer, and Christian Kral, "A Detailed Heat and Fluid Flow Analysis of an Internal Permanent Magnet Synchronous Machine by means of Computational Fluid Dynamics," IEEE Trans. Ind. Electron., vol.59,no.12, December 2012.
14. Yulia Alexandrova, Robert Scott Semken and Juha Pyrhönen, "Permanent magnet synchronous generator design solution for large direct-drive wind turbines: Thermal behavior of the LC DD-PMSG", Applied Thermal Engineering, Vol.65, No.2, pp.554-563, 2014
15. Li Liu, Wenxin Liu, David A. Cartes, "Particle swarm optimization-based parameter identification applied to permanent magnet synchronous motors" ,Engineering Applications of Artificial Intelligence, Vol.21, No.7, pp.1092-1100, 2008
16. Radhika. S, Marsalin Beno. M, Jaikumar. R.A, "Intelligent Control Design of PMSM Servo Drive" in "National Journal on Computing and Management" Volume 4, Issue No.1, pp.32-40 April 2013.